

Spectral Correlation in Incommensurate Multi-Walled Carbon Nanotubes

K.-H. Ahn,¹ Yong-Hyun Kim,² J. Wiersig,³ and K. J. Chang^{2,4}

¹ School of Physics, Seoul National University, Seoul 151-742, Korea

² Department of Physics, Korea Advanced Institute of Science and Technology, Daejeon 305-701, Korea

³ Max Planck Institute for Physics of Complex Systems,
Nöthnitzer Strasse 38, Dresden 01187, Germany

⁴ School of Physics, Korea Institute for Advanced Study, Seoul 130-012, Korea

(Dated: May 21, 2019)

We investigate the energy spectra of clean incommensurate double-walled carbon nanotubes, and find that the overall spectral properties are described by the so-called critical statistics of Anderson metal-insulator transition. In the energy spectra, there exist three different regimes characterized by Wigner-Dyson, Poisson, and semi-Poisson distributions. This feature implies that the electron transport in incommensurate multi-walled nanotubes can be either diffusive, ballistic, or intermediate between them, depending on the position of the Fermi energy.

PACS numbers: 03.65.-w, 72.15.-v, 73.23.-b

Carbon nanotubes have attracted great attention due to their remarkable electrical and mechanical properties [1]. Many theoretical and experimental studies have demonstrated that single-walled nanotubes (SWNTs) exhibit ballistic electron conduction [2, 3], and single-molecule devices utilizing semiconducting SWNTs have been realized [4]. On the other hand, despite useful applications of multi-walled nanotubes (MWNTs) [5], the transport properties of MWNTs are not well understood and even controversial; conductance measurements using scanning probe microscope showed ballistic behavior [6], while magnetoresistances measured for MWNTs on top of metallic gate indicated diffusive conduction [7, 8].

In general, MWNTs have very complex electronic structure, so that a direct use of their transport properties is severely hindered. If concentric carbon shells are especially incommensurate, the Bloch theorem is no longer valid, and the Landauer formula for conductance is not applicable because it is difficult to count the number of conducting channels [9]. In fact, several experiments on MWNTs indicated that carbon shells have often different periodicities [10, 11]. However, electronic structure calculations have been mostly focused for commensurate multi-walled nanotubes so far. Here, instead of directly calculating conductances, we investigate the *spectral properties* of energy levels in incommensurate MWNTs.

The spectral analysis of energy levels has proven to be a useful tool to probe the nature of eigenstates in disordered conductors [12]. In the diffusive metallic regime, the statistics of spectral fluctuations around a mean value is described by the Gaussian orthogonal ensemble (GOE) of random-matrix theory [13]. In this regime, the distribution $P(s)$ of energy spacings between nearest levels is well fitted by the Wigner-Dyson surmise $P_{\text{GOE}}(s) = \frac{\pi}{2} s \exp(-\frac{\pi}{4} s^2)$, where s is in units of mean level spacing Δ . In the insulating regime, where the energy levels are uncorrelated, $P(s)$ is given by the Poisson

distribution, $P_P(s) = \exp(-s)$. At the Anderson transition point, a critical statistics was found [14], and later described by semi-Poisson distribution [12], which has now been an important issue in quantum chaotic systems [15, 16, 17].

In this Letter we make a spectral analysis of the energy levels of clean incommensurate MWNTs, and find that the level statistics is similar to that of the Anderson metal-insulator transition. The energy spectra exhibit both the Wigner-Dyson and Poisson distributions in the metallic and insulating regimes, respectively, depending on the position of the Fermi level. In addition, we demonstrate that incommensurate MWNTs have an intermediate regime, which satisfies the semi-Poisson statistics.

To investigate the spectral correlation, we consider double-walled carbon nanotubes (DWNTs), because the electrical conduction in MWNTs is believed to be governed by the outermost shells [8, 18]. We use a tight-binding model with one π -orbital per carbon atom, which successfully describes the electronic structure of DWNTs [19, 20]. The tight-binding Hamiltonian is given by

$$H = \gamma_0 \sum_{i,j} c_j^\dagger c_i - W \sum_{i',j'} \cos(\theta_{i'j'}) e^{(a-d_{i'j'})/\delta} c_{j'}^\dagger c_{i'}, \quad (1)$$

where γ_0 (= -2.75 eV) is the hopping parameter between intra-layer nearest neighbor sites, i and j , and W (= $\gamma_0/8$) is the strength of inter-wall interactions between inter-layer sites, i' and j' , with the distance of $d_{i'j'}$ and the cut-off for $d_{i'j'} > 3.9$ Å. Here θ_{ij} is the angle between two π orbitals, $c_{i'}$ is the annihilation operator of an electron on site i' , a (= 3.34 Å) is the distance between two carbon walls, and $\delta = 0.45$ Å.

The two shells of DWNTs are incommensurate if the ratio of the unit cell lengths along the tube axis is irrational. We test many incommensurate DWNTs, where both the shells are metallic or semiconducting, a semiconducting shell is inside a metallic tube, and vice versa. Since the spectral properties are similar for all the tubes

Fig. 1 Ahn, et al.

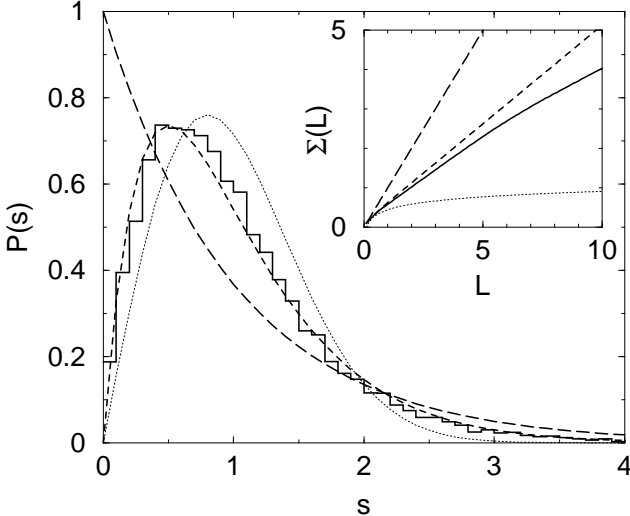


FIG. 1: The nearest energy spacing distribution $P(s)$ (solid) for 20220 energy levels between -7 and 7 eV and the semi-Poisson (dashed), Poisson (long-dashed), and GOE (dotted) distributions. The inset shows the number variance $\Sigma(L)$.

considered here, we only present the spectral properties of the (16,5)/(23,8) DWNT, where the semiconducting (16,5) single-walled tube is aligned inside the metallic (23,8) tube. The diameters of the inner and outer tubes are 1.5 and 2.2 nm, respectively, and the nanotube length is set to be about 53 nm.

To extract the fluctuations from the level sequence, it is customary to map the real energy spectra $\{\epsilon_i\}$ onto the unfolded spectra $\{E_i\}$ through $E_i = \bar{N}(\epsilon_i)$, where $\bar{N}(\epsilon_i)$ is the number of levels up to ϵ_i and the overline denotes its broadened value [21]. Here we use the Gaussian broadening scheme for averaging the energies [22]. After unfolding, we obtain the distribution $P(s)$ as a function of nearest energy spacing, $s_i = E_i - E_{i-1}$ (the mean level spacing of the unfolded spectra equals 1), and the number variance $\Sigma(L) = \langle (n(L, E) - L)^2 \rangle$, which represents the variance of the number of levels in the interval $(E - L/2, E + L/2)$, i.e., $n(L, E) = \bar{N}(E + L/2) - \bar{N}(E - L/2)$. The bracket $\langle \dots \rangle$ denotes the average around the energy E on an energy window much larger than the mean level spacing but much smaller than E .

Figure 1 shows the calculated $P(s)$ and $\Sigma(L)$ for the (16,5)/(23,8) nanotube on the energy window from -7.0 to 7.0 eV, where 20220 levels exist. We find that $P(s)$ and $\Sigma(L)$ can not be described by the Poisson distribution or GOE, but, they are well described by the semi-Poisson (SP) distribution [15, 16, 17];

$$P_{SP}(s) = 4s \exp(-2s) \quad (2)$$

$$\Sigma_{SP}(L) = \frac{L}{2} + \frac{1}{8}(1 - e^{-4L}). \quad (3)$$

The SP distribution is defined by removing every other

level from an ordered Poisson sequence and turned out to be a good fit to the critical statistics of several disordered systems like the Anderson model at mobility edge [14, 23], and also of other systems without disorder such as pseudo-integrable quantum billiards [16, 17, 24]. Up to now, it is still unresolved why the semi-Poisson distribution appears in those systems.

While $P(s)$ carries information on short-range correlation in the energy spectra, $\Sigma(L)$ contains rather long-range correlation. Usually $\Sigma(L)$ indicates a deviation from the universal value for large L , thus, the particle dynamics becomes nonuniversal at short time scale. For large L , the spectral correlation is not universally semi-Poisson but depends on the helicity of nanotubes. The deviation from the SP distribution gives useful information; the linear behavior for large L , i.e., $\Sigma(L)/L \rightarrow \chi$, represents the level compressibility, and for disordered metals χ was shown to be [25]

$$\chi = \frac{1}{2} \left(1 - \frac{D_2}{d} \right), \quad (4)$$

where D_2 is the multifractal exponent of the inverse participation ratio and d is the spatial dimension. Here D_2/d is related to the 'probability of return' [26],

$$p(t) \propto t^{-D_2/d}. \quad (5)$$

Our incommensurate DWNTs behave as two-dimensional systems ($d = 2$) with the off-diagonal disorder, which has a mixed boundary between periodic and hard-wall conditions. From the inset in Fig. 1, we estimate D_2/d to be about 0.32 for the DWNT considered here. While $p(t) \propto t^{-d/2}$ in normal diffusion, our system exhibits anomalous diffusion, which was also found by previous wavepacket spreading calculations [20].

The semi-Poisson distribution in Fig. 1 is mostly contributed from the region of large $|E|$, where the density of states (DOS) is high, while the energy statistics is usually not independent of the energy regime. Since real electron conductances occur near the Fermi level, it is instructive to examine the energy-level statistics on various energy windows. Although we discuss the level statistics when the Fermi level increases, we find similar statistics for the downward shift of the Fermi level, which usually occurs in hole-doped tubes.

In the level statistics, we remove the states lying between 0 and 0.08 eV, which are associated with the localized states near the sample boundary due to the finite size of the system. In Fig. 2(a), $P(s)$ is drawn for low energy states from 0.08 to 1.3 eV, and exhibits the Poisson distribution, indicating that the energy levels are uncorrelated. Single-wall nanotubes, which are constituents of the DWNT, are approximately described in terms of $P_P(s)$ and $\delta(s)$. In this case, the delta-function peak results from the doubly degenerate states due to inversion symmetry. If inter-wall interactions are absent in the

DWNT, a superposition of two independent spectra of the nanotube constituents is also described by the Poisson and delta functions.

When inter-wall interactions break the degeneracy, smearing out the delta-function peak, $P(s)$ is still Poisson-like, as shown in Fig. 2(a), implying that the energy mixing between the two carbon shells is insignificant for low energies. In the low energy regime, it is useful to use the Landauer formula,

$$G = \frac{2e^2}{h} \sum_i T_i(E_F), \quad (6)$$

where $T_i(E_F)$ is the transmission probability of the channel i at the Fermi energy E_F [9]. Our results infer that quantized conductances observed in MWNTs [6] may be due to the fact that the Fermi level is close to the charge neutrality point, $E_F \approx 0$. However, it is usually very difficult to find experimentally the location of the Fermi level.

As the Fermi level is shifted further, since the DOS increases and the mean level spacing becomes smaller, inter-wall interactions induce a more significant mixing of the energy levels between the carbon shells. For higher energy states, we find that $P(s)$ follows the SP distribution, as shown in Figs. 2(b) and (d). The quantum conductivity in this regime still remains a challenging problem, because it is not known how to describe the interference effects on the electron path as well as the time-reversal path. It is not guaranteed whether the usual weak localization formula, $\delta\sigma \propto -\int_{\tau}^{\tau_{\phi}} dt p(t)$, is valid in this regime, where τ_{ϕ} is the dephasing time and τ is the elastic mean free time.

In Fig. 2(c), one can see that the SP distribution evolves to the GOE as going to the energy region, where $P(s)$ is quite close to the Wigner-Dyson surmise. We also find the GOE-like statistics for both $P(s)$ and $\Sigma(L)$ in all the incommensurate DWNTs tested here. The appearance of the GOE-like behavior indicates that all the symmetries except for time-reversal symmetry are effectively broken, and electron motion is well described by diffusive motion. It is interesting to note that there is a diffusive regime in systems without any impurity. In this regime, the conductivity of MWNTs may be described by the weak localization theory. One should also note that the weak localization theory is applicable for energies higher than those in the first SP regime, because the sequence of statistics with increasing energy is

$$\text{Poisson} \rightarrow \text{SP} \rightarrow \text{GOE} \rightarrow \text{SP}.$$

In MWNTs on top of metallic gates, the details of contacts, local excessive charges, and depletion of charge carriers may change the position of the Fermi level [27]. Based on our results, we guess that in conductance measurements [2, 4, 8], the Fermi level is shifted to the GOE

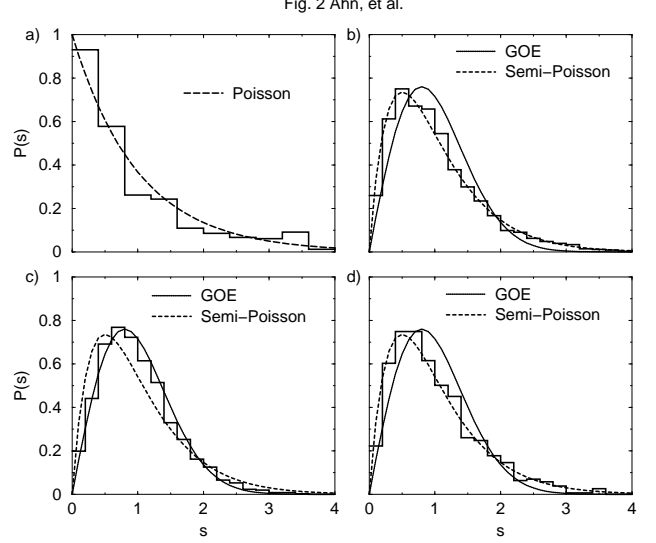


FIG. 2: The nearest energy spacing distribution $P(s)$ on the energy windows of (a) $(0.08, 1.3\text{eV})$ with 511 levels, (b) $(1.0, 2.5\text{eV})$ with 1872 levels, (c) $(2.5, 3.5\text{eV})$ with 2696 levels, and (d) $(3.5, 4.0\text{eV})$ with 888 levels.

regime or to the SP regime (close to the GOE) where conductivity is properly described by the weak localization formula. If the Fermi level lies in that SP regime, the small periodic oscillation observed by magnetoconductance measurements [8], which can not be reconciled with the weak localization theory, might be a non-universal fingerprint of interferences between certain long trajectories in the SP regime. Further theoretical effort is needed for this issue.

The calculated variances over every 1000 consecutive levels are compared with the densities of states for two different DWNTs in Fig. 3. The size of fluctuations of the level spacing is dictated by the spectral statistics;

$$\begin{aligned} \langle (s - \langle s \rangle)^2 \rangle &= \int_0^{\infty} ds (s - 1)^2 P(s) \quad (7) \\ &= 1, \frac{1}{2}, \frac{4}{\pi} - 1 \quad (\text{Poisson, SP, GOE}). \end{aligned}$$

It is expected that the effect of inter-wall interactions on the level spacing is most significant when the mean level spacing Δ is minimum near $E = \pm\gamma = \pm 2.75\text{eV}$, where the maximum DOS occurs on a graphene sheet. One can see $\langle (s - \langle s \rangle)^2 \rangle = \frac{4}{\pi} - 1 \approx 0.27$ near $E = \pm\gamma = \pm 2.75\text{eV}$, which is a signature of GOE distribution. The variances larger than 1 near $E = 0$ are due to the fact that $P(s)$ is not completely Poisson-like because the degenerate levels of each nanotube layer are not completely lifted up.

We find that a transition from the Poisson-like to SP-like statistics occurs at lower energies as the diameter of nanotubes increases. One of the reasons for this trend seems that the DOS is enhanced for nanotubes with larger diameters. The transition energy is close to 1 eV in the $(43,8)/(51,9)$ DWNT with the outer and inner di-

Fig. 3 Ahn, et al.

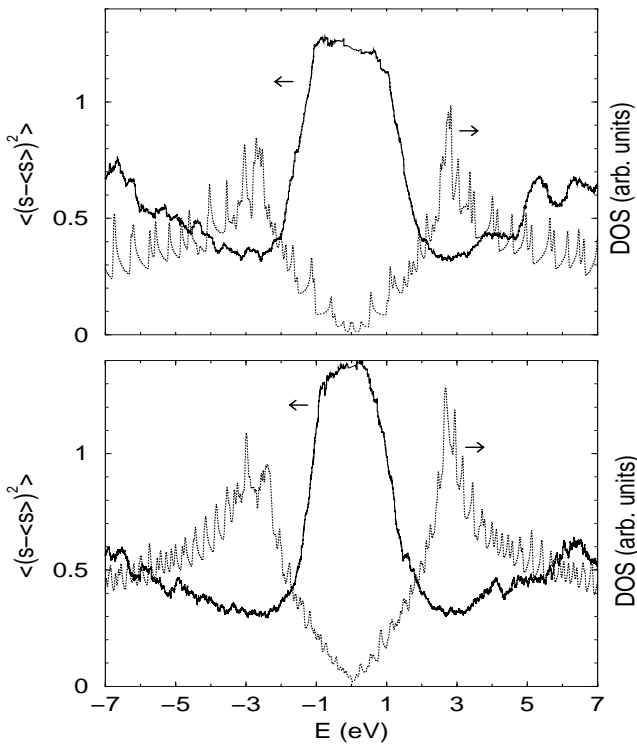


FIG. 3: The variance of the level spacing (solid) in Eq. (7) and the density of states (dotted) in arbitrary units for the (16,5)/(23,8) (upper panel) and (43,8)/(51,9) (lower panel) double-walled tubes.

ameters of 4.4 and 3.7 nm, respectively, while it is higher than 1 eV for the (16,5)/(23,8) tube with the diameters of 2.2 and 1.5 nm, as shown in Fig. 3. Since experimentally measured diameters of MWNTs are often in the range of 10 nm, we expect that the crossover of spectral statistics occurs at energies lower than 1 eV.

Finally, we point out that the spectral statistics might be probed through conductance measurements in the Coulomb blockade regime [28]. In this case, temperature should be low enough to ensure that $k_B T < U, \Delta$, where U is the charging energy of nanotube dot. In the resonant tunneling regime, where electron tunnels through one quantum level, if electron-electron interactions are not too strong [29], the conductance peak spacing with varying the gate voltage provides information on the single-particle energy spacing, $\epsilon_i - \epsilon_{i-1}$. The variance expected from Eq. (7) and Fig. 3 might be useful to test the single-electron nanotube transistor in the resonant tunneling regime.

In conclusion, we have shown that the spectral statistics of incommensurate double-walled nanotubes follows the Poisson, GOE, or SP distribution, depending on the energy window, while the overall states are well described by the SP. This results indicate that the nature of elec-

tron transport in multi-walled nanotubes can be either ballistic, diffusive, or critical, depending on the position of the Fermi level. It is questioned whether the weak localization correction is relevant to existing experiments. The Coulomb blockade oscillation in nanotube dots is suggested to investigate the spectral statistics in this work.

The authors acknowledge Professors J. Ihm and J. Yu for useful discussions. This work was supported by QSRC and BK21.

[1] R. Saito, G. Dresselhaus, and M.S. Dresselhaus, *Physica Properties of Carbon Nanotubes* (Imperial College Press, London, 1998).

[2] S.J. Tans *et al.*, *Nature (London)* **386**, 474 (1997).

[3] M. Bockrath *et al.*, *Science* **275**, 1922 (1997).

[4] S.J. Tans *et al.*, *Nature (London)* **393**, 49 (1998); R. Martel *et al.*, *Appl. Phys. Lett.* **73**, 2447 (1998).

[5] K. Tsukagoshi *et al.*, *Nature (London)* **401**, 572 (1999).

[6] S. Frank *et al.*, *Science* **280**, 1744 (1998).

[7] L. Langer, *Phys. Rev. Lett.* **76**, 479 (1996).

[8] A. Bachtold *et al.*, *Nature* **397**, 673 (1999).

[9] S. Datta, *Electronic Transport in Mesoscopic Systems* (Cambridge University Press, Cambridge, 1995).

[10] S. Iijima, *Nature (London)* **354**, 56 (1991).

[11] M. Ge and K. Sattler, *Science* **260**, 515 (1993).

[12] For example, see G. Montambaux, in *Quantum Fluctuations*, Proceedings of the Les Houches Summer School, Session LXIII, edited by E. Giacobino *et al.* (Elsevier, Amsterdam, 1996).

[13] M.L. Mehta, *Random Matrices and the statistical theory of energy levels* (Academic Press, New York, 1967).

[14] B.I. Shklovskii *et al.*, *Phys. Rev. B* **47**, 11487 (1993).

[15] H. Hernández-Saldaña *et al.*, *Phys. Rev. E* **60**, 449 (1999).

[16] E.B. Bogomolny *et al.*, *Phys. Rev. E* **59**, 1315 (1999).

[17] E.B. Bogomolny *et al.*, *Eur. Phys. J. B* **19**, 121 (2001).

[18] P. G. Collins *et al.*, *Science*, **292**, 706 (2001).

[19] R. Saito *et al.*, *J. Appl. Phys.* **73**, 494 (1993); J.C. Charlier and J.P. Michenaud, *Phys. Rev. Lett.* **70**, 1858 (1993).

[20] S. Roche *et al.*, *Phys. Rev. B* **64**, 121401 (2001).

[21] F. Haake, *Quantum signatures of chaos* (Springer, Berlin, 1991).

[22] J.M.G. Gómez *et al.*, arXiv:nlm.CD/0112014, (2001).

[23] D. Braun *et al.*, *Phys. Rev. Lett.* **81**, 1062 (1998) and references therein.

[24] J. Wiersig, *Phys. Rev. E* **65**, 046217 (2002).

[25] J.T. Chalker *et al.*, *Pis'ma Zh. Eksp. Teor. Fiz.* **64**, 335 (1996) [JETP Lett. **64**, 388 (1996)].

[26] J.T. Chalker *et al.*, *Phys. Rev. Lett.* **77**, 554 (1996).

[27] Y. Xue and S. Datta, *Phys. Rev. Lett.* **83**, 4844 (1999).

[28] M.T. Woodside and P.L. McEuen, *Science* **296**, 1098 (2002).

[29] K.-H. Ahn *et al.*, *Phys. Rev. Lett.* **83**, 4144 (1999).